

FIG. 2. G versus square of momentum transfer t , in units of $2 F^{-2}$, where G^2 is proportional to the total cross section proton-antiproton annihilation into electron-positron pairs, taken from Table III. The point is a measurement from Ref. 18.

The values of G , A , and $\sin\phi$ are presented in Table III for t in the annihilation region. In Fig. 2 we compare our G values with the one measured point¹⁸ of $G=2.2$

¹⁸ M. Conversi, T. Massam, Th. Muller, and A. Zichichi, Phys.

at $t=86$ and fair agreement is observed.¹⁹ The values of $\sin\phi$ are extremely small due to the restricted form of the input function and the constraints at $t=45$.

An approach identical to the one presented here is now being applied to the simultaneous analysis of the neutron and proton data. It is hoped that a self-consistent four-pole fit will emerge with the important resonances having the more physical characteristics of widths.

ACKNOWLEDGMENTS

The author wishes to thank Dr. M. Razavy for suggesting this work and also R. Teshima for help with the computer calculations.

Letters 5, 195 (1963); *Proceedings of the Sienna International Conference on Elementary Particles, 1963*, edited by G. Bernadini and G. P. Puppi (Società Italiana di Fisica, Bologna, 1963).

¹⁹ The one other determination (Ref. 8) of this plot has identical shape but occurs just above the data point. A few points are $t=45$, $G=3.4$; $t=83$, $G=2.4$; and $t=400$, $G=1.6$.

Photoproduction of Neutral K Mesons*

S. D. DRELL AND M. JACOB†

Stanford Linear Accelerator Center, Stanford University, Stanford, California

(Received 6 January 1965)

Photoproduction of a neutral K -meson beam at high energies from hydrogen is computed in terms of a K^* vector-meson exchange mechanism corrected for final-state interactions. The results are very encouraging for the intensity of high-energy K_2 beams at high-energy electron accelerators. A typical magnitude is $20 \mu\text{b/sr}$ for a lower limit of the K^0 photoproduction differential cross section, at a laboratory peak angle of 2° , for 15-BeV incident photons.

INTRODUCTION

WE compute the cross section for photoproduction of K^0 mesons at high energies

$$\gamma + p \rightarrow K^0 + \Sigma^+ \quad (1)$$

due to the mechanism illustrated in Fig. 1, i.e., via K^* exchange. Our purpose is to obtain an estimate for the neutral K beam which may be produced with high-energy electron machines. There is now experimental evidence that vector-meson exchange plays an important role in high-energy two-body or quasi-two-body reactions.¹ Furthermore, in reaction (1) the K^* meson is the lightest particle with the quantum numbers of the t channel, since there is no K^0 current. We thus

expect K^* exchange to be a dominant feature in high-energy K^0 photoproduction.

Nevertheless, one should not be satisfied with a simple Born-approximation calculation as illustrated by Fig. 1. In order to reproduce experimental data in the 2–4-BeV range, the one-meson-exchange approximation has to be corrected to take proper care of the existence of many competing channels. This correction has been applied with great success by Gottfried and Jackson² and other authors to several reactions. The method used is the distorted-wave Born approximation, currently applied in low-energy nuclear physics. Each partial-wave amplitude F_j is obtained from the Born-approximation partial-wave contribution B_j , through the following

* Work supported in part by U. S. Atomic Energy Commission.
† On leave of absence from Service de Physique Theorique, Saclay, Gif-sur-Yvette, France.

¹ J. D. Jackson, Rev. Mod. Phys. (to be published).

² K. Gottfried and J. D. Jackson, Nuovo Cimento 34, 735 (1964); A. Dar and W. Tobocman, Phys. Rev. Letters 12, 511 (1964); L. Durand and Y. T. Chiu, *ibid.* 12, 399 (1964); M. H. Ross and G. L. Shaw, *ibid.* 12, 627 (1964).

relation:

$$F_j(s) = e^{i\delta_{jf}(s)} B_j(s) e^{i\delta_{ji}(s)}, \quad (2)$$

where δ_{jf} and δ_{ji} are the scattering phase shifts (generally complex) for angular momentum j in the final and initial states; s stands for the c.m. energy squared. This method provides an answer free of adjustable parameters when the elastic-scattering amplitudes for the initial and final two-body systems are purely imaginary. The inelasticity parameters $\eta_j = |e^{2i\delta_j}|$ can then be obtained from the shape of the elastic diffraction peak and the total cross section.

It must be pointed out though that this distorted-wave approximation, as expressed by (2), does not in general have a firm theoretical basis in application to high-energy reactions. Where it is valid, as has been recently shown by Omnes,³ is for partial waves with inelasticity parameters that are not too different from unity. Nevertheless, if (2) is not formally correct for low partial waves, where the absorption is large, it does give the correct qualitative behavior of a strong damping of the two-body reaction amplitude due to the effect of many open competing channels. In other words, we expect the statistical model to be more reliable than the one-meson-exchange approximation when calculating the low partial-wave amplitudes. Since there are so many open channels, these particular two-body channels of low angular momentum should enter with a small amplitude and not play a dominant role in the total amplitude.

We do not expect then that (2), used for all partial waves, will give a result much different from what could be obtained with a more refined procedure, and it should be adequate in order to yield an estimate of the cross section. In particular, we present results corresponding to the maximum possible absorption (no S wave at all) in this formalism in order to make a pessimistic estimate of the K^0 beam intensity.

This treatment protects unitarity in the incident and outgoing channels by including the possibility of transition to all the open inelastic channels, as first discussed by Sopkovich and Baker and Blankenbecler.⁴ Its main effect is to reduce the Born-approximation predictions and to make the angular distribution more strongly peaked at small angles.

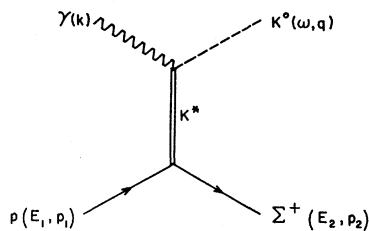


FIG. 1. K^* exchange in photoproduction.

³ R. Omnes, Phys. Rev. **137**, B649 (1965).

⁴ N. T. Sopkovich, Nuovo Cimento **26**, 186 (1962); M. Baker and R. Blankenbecler, Phys. Rev. **128**, 415 (1962).

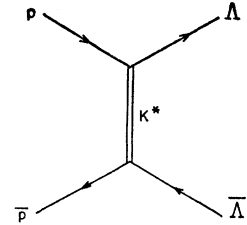


FIG. 2. K^* exchange in $p\bar{p}$ collision.

In the photoproduction process, the corrections come only from the strong final-state interactions. Equation (2) is then replaced by ($\eta_{ji} \approx 1$)

$$F_j(s) = [\eta_j(s)]^{1/2} B_j(s). \quad (3)$$

To obtain the photoproduction cross section for K^0 mesons we must still insert values for the $K^*K^0\gamma$ coupling constant, or the K^{0*} radiative decay width, as well as for the $K^*p\Sigma$ coupling constant in the B_j amplitudes, and for the $K\Sigma$ elastic-scattering angular distribution and total cross section for the absorption factor η_j . In order to obtain a reliable order of magnitude we may with some confidence use SU_3 symmetry to relate these parameters to already known quantities. We can, in this way, make predictions for the K^0 photoproduction cross section in terms of "experimental" parameters.

Our calculation follows the same lines as one already carried out for the $p\bar{p} \rightarrow \Lambda\bar{\Lambda}$ reaction in the 2–4 BeV range. In this process K^* exchange⁵ dominates, as shown in Fig. 2, but with the low partial waves absorbed out using the model of Gottfried and Jackson. An extremely good fit to the experimental data is obtained assuming identical inelasticity parameters for the $p\bar{p}$ and $\Lambda\bar{\Lambda}$ channels and a $K^*p\Lambda$ coupling constant obtained from the ρ -nucleon coupling constant by SU_3 symmetry.

Although this strengthens our confidence in the model, one must be aware of the fact that we want to obtain a cross-section estimate for (1) at energies ranging from 10 to 20 BeV, which are much higher than the energy range in which it has proved successful (2–4 BeV). In using this approximation we assume that the vector-meson-exchange contribution remains the dominant feature when the energy increases.

Our motivation in carrying out this calculation is to emphasize the strong suggestion that an intense "healthy" K_2 beam will emerge from high-energy electron accelerators (SLAC in particular) and will be available for detailed experimental studies.

In the spirit of making such an experimental prediction we shall bias the calculations in the following section so as to yield a lower limit prediction by overemphasizing absorption from the final $K^0\Sigma^+$ channel. The final results are shown graphically in Figs. 3–6. They illustrate the reduction from the simple

⁵ G. Cohen and H. Navelet, Nuovo Cimento (to be published).

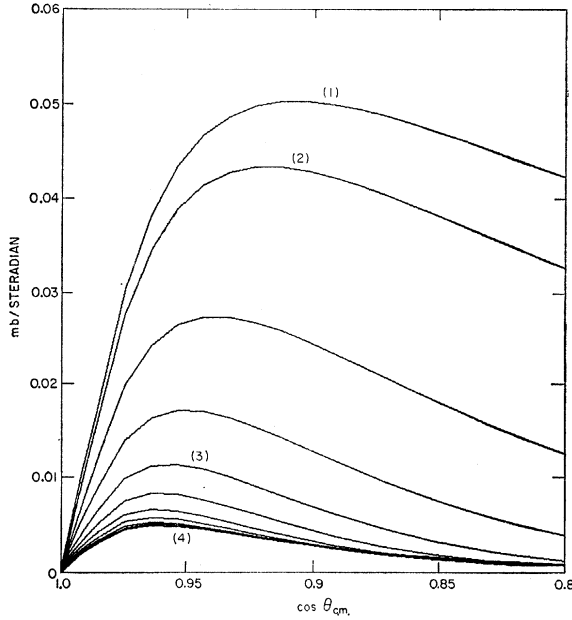


FIG. 3. Center-of-mass differential cross section at 10 BeV. Curve (1) gives the Born approximation. Curve (2) is obtained after subtraction of the $j = \frac{1}{2}$ partial wave. Curves (3) and (4) are respectively obtained after the $j = \frac{1}{2}, \frac{3}{2}, \frac{5}{2}, \frac{7}{2}$, and all partial waves have been corrected for absorption in final state. The results are shown as directly obtained from and drawn by the computer.

one-particle exchange amplitude when absorption is taken into account in the individual partial waves.

CALCULATIONS

In the simple one-particle exchange approximation the amplitude for Fig. 1 with the indicated kinematics

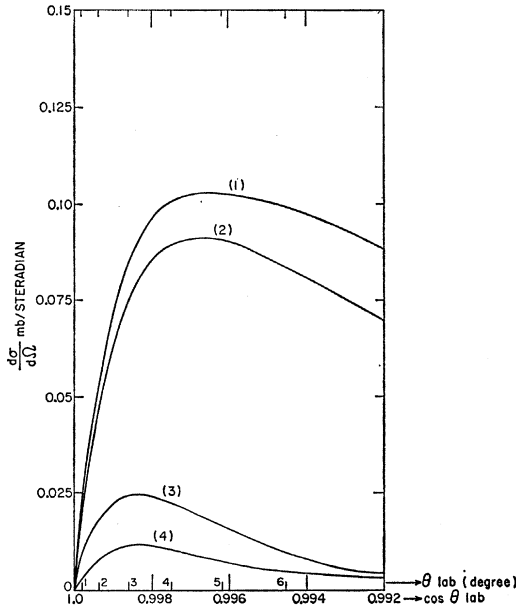


FIG. 4. Laboratory differential cross section at 10 BeV. Curves (1), (2), (3), and (4) refer to the same steps as on Fig. 3.

is written

$$\mathfrak{M} = g_{K^*K\gamma} \frac{g_{K^*p\Sigma}}{m^*} \left(\frac{M_N M_\Sigma}{4k\omega E_1 E_2} \right)^{1/2} \times (2\pi)^4 \delta(q + p_2 - p_1 - k) F, \quad (4)$$

where

$$F = \frac{\epsilon_{\mu\nu\sigma\tau} \epsilon^\mu k^\nu q^\sigma \{ \bar{u}(p_2) \gamma^\tau u(p_1) \}}{(q-k)^2 - m^{*2}}, \quad (5)$$

ϵ is the photon polarization vector, m^* denotes the K^* mass, and M_N and M_Σ the nucleon and Σ mass, respectively. The $K^*K\gamma$ vertex with the coupling constant $g_{K^*K\gamma}$ has the unique form shown by the antisymmetric outer product in the numerator of (5), up to a form factor depending on momentum transfer $t = (q-k)^2$. This form-factor dependence on t is neglected here. In the region of interest at the peak of the differential cross section $|t| \approx m^{*2}$. The relation of $g_{K^*K\gamma}$ to the radiative decay width $\Gamma_{K^* \rightarrow K\gamma}$ is given by

$$\frac{g_{K^*K\gamma}^2}{4\pi} = \frac{24\Gamma_{K^* \rightarrow K\gamma}}{m^*(1 - m^2/m^{*2})^{3/2}}, \quad (6)$$

where m stands for the K mass. The coupling strength at the $K^*p\Sigma$ vertex $g_{K^*p\Sigma} \bar{u}(p_2) \gamma_\mu u(p_1)$ is denoted by $g_{K^*p\Sigma}$. A Pauli-type coupling is neglected as relatively unimportant when computing the magnitudes of differential cross sections for low momentum transfers.

The differential cross section in the center-of-mass system for unpolarized particles is given by

$$\left(\frac{d\sigma}{d\Omega} \right)_{c.m.} = \frac{q M_N M_\Sigma}{k W^2 m^{*2}} \left(\frac{g_{K^*K\gamma}^2}{4\pi} \right) \left(\frac{g_{K^*p\Sigma}^2}{4\pi} \right) \times \frac{1}{2} \sum_{\text{Pol}} \frac{1}{2} \sum_{\text{Spin}} |F|^2, \quad (7)$$

where W denotes the total energy.

Direct calculation of (4), (5), and (7) gives an upper limit in the absence of final-state interaction, and we quote the result here in order to provide a general orientation. In the laboratory system and in the limit of small angles and high energies, we find

$$\lim_{M/k \rightarrow 0, \theta \rightarrow 0} \left(\frac{d\sigma}{d\Omega} \right)_{\text{lab}} = \frac{1}{2m^{*2}} \left(\frac{g_{K^*p\Sigma}^2}{4\pi} \right) \left(\frac{g_{K^*K\gamma}^2}{4\pi} \right) \times \frac{\theta_{\text{lab}}^2}{[\theta_{\text{lab}}^2 + m^{*2}/k_{\text{lab}}^2]^2}. \quad (8)$$

Putting $g_{K^*p\Sigma}^2/4\pi \sim 1$ and $g_{K^*K\gamma}^2/4\pi \sim 1/137$, as becomes an electromagnetic transition corresponding to a radiative decay width ~ 0.1 MeV in (6), we find at the peak angle $\theta_{\text{lab}} = m^*/k_{\text{lab}}$ and at an incident photon energy of $k_L = 15$ BeV,

$$(d\sigma/d\Omega)_{\text{peak}} \approx 100 \mu\text{b/sr}. \quad (9)$$

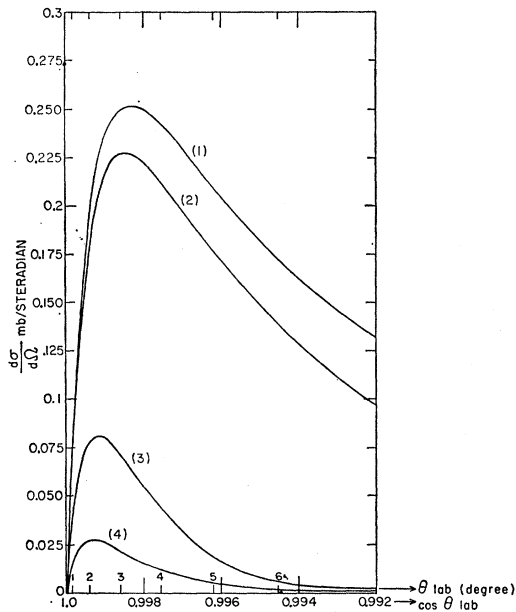


FIG. 5. Laboratory differential cross section at 15 BeV. Curves (1), (2), (3), and (4) refer to the same steps as on Fig. 4.

We can compute with this production cross section the K_2 yield with an incident beam intensity of 20-BeV electrons of 10^{14} /sec as predicted for SLAC. Through a $\frac{1}{2}$ radiation length target there will emerge 5×10^{13} dk/k

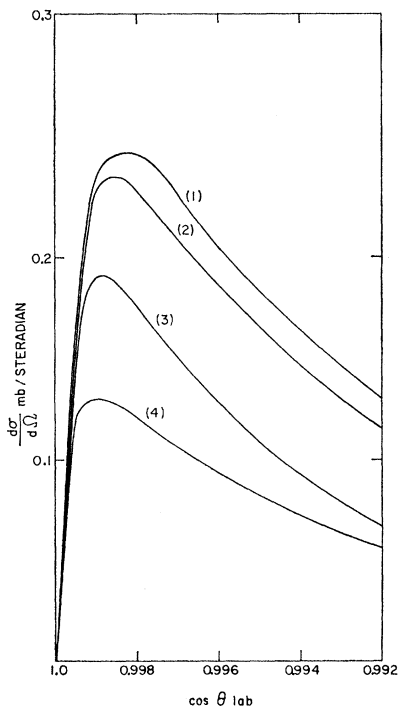


FIG. 6. Laboratory differential cross section at 15 BeV. Curves (1), (2), (3), and (4) refer to the same steps as on Fig. 4. The absorption is not assumed to be complete in the S wave but given by Eqs. (18) and (12).

photons per second in an energy interval dk about k , or 3×10^{13} photons/BeV-sec at 15 BeV. If these photons are incident on an 8 g/cm^2 hydrogen target the resulting long-lived K_2 flux is 10^6 /sec within a solid angle of $\frac{1}{10}\pi (m^{*2}/k^2) \approx 10^{-3}$ sr about $\theta = m^*/k \approx 3^\circ$.

In analyzing the effect of final-state interactions it has been found to be necessary to treat the particle spins correctly in order to avoid unphysical diffraction bumps in the calculated angular distributions. Since our primary interest here is in the formation of a secondary beam of K_2 's of high flux and in view of uncertainties in the coupling constants $g_{K^*\Sigma p}$ and $g_{\gamma K^*K}$, it suffices to make a simple spinless impact-parameter calculation of the absorption from the $K^0\Sigma^+$ channel. The qualitative results obtained in this way are then confirmed by a detailed calculation performed by decomposing the amplitude F into individual helicity and angular-momentum channels and then absorbing each partial wave with the parameters computed from the diffraction scattering.

First we present the simple result. The peak in the differential cross section (8) occurs at the angle $\theta = m^*/k$ corresponding to a momentum transfer $k\theta = |t|^{1/2} = m^*$. This defines an impact parameter $b = 1/m^*$ and according to the distorted-wave Born approximation the final-state amplitude is diminished by the factor

$$[\eta(b)]^{1/2} = \left\{ 1 - \frac{\sigma_t(s)}{4\pi A(s)} e^{-i\pi/2 A(s)} \right\}^{1/2} \quad (10)$$

representing the fractional absorption of the $K^0\Sigma^+$ system into other channels when they collide with impact parameter b . In (10), σ_t is the $K^0\Sigma^+$ collision cross section at energy \sqrt{s} , and the approximation is made that the amplitude for $K^0\Sigma^+$ scattering is imaginary, i.e.,

$$-if(s,0) = \text{Im}f(s,0) = (k/4\pi)\sigma_t(s),$$

and that for small finite momentum transfer, the amplitude is parametrized as

$$f(s,t) = e^{-\frac{1}{2}At} f(s,0). \quad (11)$$

A as well as σ_t are fit to π -nucleon high-energy scattering parameters. Using 15-BeV data, so that⁶

$$\sigma_t = 27 \text{ mb} \quad \text{and} \quad A = 10/(\text{BeV})^2, \quad (12)$$

we evaluate from (10) for $b = 1/m^*$,

$$\eta^{1/2}(b = 1/m^*) = 0.7.$$

This gives a reduction from the peak of $100 \mu\text{b/sr}$ evaluated in (9) by a factor of only $\frac{1}{2}$

$$\frac{d\sigma}{d\Omega} = 100\eta \left(\frac{1}{m^*} \right) = 50 \mu\text{b/sr}. \quad (13)$$

For a lower limit to the production cross section we may

⁶ K. J. Foley *et al.*, Phys. Rev. Letters **11**, 425 (1963); S. Brandt *et al.*, *ibid.* **10**, 413 (1963).

set to unity the coefficient in (10), i.e., replace $\sigma_i/4\pi A$ by 1 in (10) corresponding to complete absorption of the S -wave amplitude. This would reduce (9) then by a factor 16 down to $6 \mu\text{b}/\text{sr}$. However, this is only a rough approximation of the effect since the peak also moves to a smaller angle.

$$F = \begin{pmatrix} F_1 \\ F_2 \\ F_3 \\ F_4 \end{pmatrix} = \frac{1}{2\sqrt{2}} \left(\frac{E_1 + M_N}{2M_N} \right)^{1/2} \left(\frac{E_2 + M_\Sigma}{2M_\Sigma} \right)^{1/2} \frac{1}{\cos\theta - V} \begin{Bmatrix} -2e^{-i\varphi/2} \sin(\theta/2) [(1 + \omega/q)(r_1 + r_2) + (1 - r_1)(1 - r_2) \cos^2(\theta/2)] \\ e^{3i\varphi/2} \sin\theta \sin(\theta/2) (1 + r_1)(1 - r_2) \\ e^{3i\varphi/2} \sin\theta \cos(\theta/2) (1 + r_1)(1 + r_2) \\ -2e^{-i\varphi/2} \cos(\theta/2) [(1 - \omega/q)(r_1 - r_2) + (1 + r_2)(1 - r_1) \sin^2(\theta/2)] \end{Bmatrix}, \quad (14)$$

where

$$V \equiv -\frac{\omega}{q} + \frac{m^*{}^2 - m^2}{2kq}, \quad r_1 \equiv \left(\frac{E_1 - M_N}{E_1 + M_N} \right)^{1/2}, \quad r_2 \equiv \left(\frac{E_2 - M_\Sigma}{E_2 + M_\Sigma} \right)^{1/2}.$$

In the high-energy limit $r_1, r_2 \rightarrow 1$ and only the first and third amplitudes above, corresponding to no helicity flip on the baryon line and to right- and left-handed incident photons, respectively, survive to leading order in M/E . The angular-momentum projections of the individual F_i are achieved with the representation coefficients of the rotation group,

$$\begin{aligned} F_1^j &= \int_{-1}^1 d(\cos\theta) F_1(\theta) d_{1/2-1/2}^j(\theta), \\ F_2^j &= \int_{-1}^1 d(\cos\theta) F_2(\theta) d_{3/2-1/2}^j(\theta), \\ F_3^j &= \int_{-1}^1 d(\cos\theta) F_3(\theta) d_{-3/2-1/2}^j(\theta), \\ F_4^j &= \int_{-1}^1 d(\cos\theta) F_4(\theta) d_{-1/2-1/2}^j(\theta); \end{aligned} \quad (15)$$

$$\begin{aligned} d_{1/2-1/2}^j(\theta) &= -\frac{\sin(\theta/2)}{j + \frac{1}{2}} (P'_{j+1/2} + P'_{j-1/2}), \\ d_{3/2-1/2}^j(\theta) &= \frac{\cos(\theta/2)}{j + \frac{1}{2}} \left(-\left(\frac{2j-1}{2j+3} \right)^{1/2} P'_{j+1/2} \right. \\ &\quad \left. + \left(\frac{2j+3}{2j-1} \right)^{1/2} P'_{j-1/2} \right), \\ d_{-3/2-1/2}^j(\theta) &= -\frac{\sin(\theta/2)}{j + \frac{1}{2}} \left(\left(\frac{2j-1}{2j+3} \right)^{1/2} P'_{j+1/2} \right. \\ &\quad \left. + \left(\frac{2j+3}{2j-1} \right)^{1/2} P'_{j-1/2} \right), \\ d_{-1/2-1/2}^j(\theta) &= \frac{\cos(\theta/2)}{j + \frac{1}{2}} (P'_{j+1/2} - P'_{j-1/2}). \end{aligned} \quad (16)$$

For a result with more quantitative meaning we return now to (5) and project out the four individual helicity amplitudes⁷ corresponding to an incident baryon of $+$ helicity ending up with $+$ or $-$ helicity with absorption of a right-handed or left-handed photon, respectively:

In terms of their partial-wave expansions the individual amplitudes are given by

$$\begin{aligned} F_1 &= \sum_{j=1/2}^{\infty} (j + \frac{1}{2}) F_1^j d_{1/2-1/2}^j(\theta) \sqrt{\eta_j} \\ F_2 &= \sum_{j=1/2}^{\infty} (j + \frac{1}{2}) F_2^j d_{3/2-1/2}^j(\theta) \sqrt{\eta_j}, \\ F_3 &= \sum_{j=1/2}^{\infty} (j + \frac{1}{2}) F_3^j d_{-3/2-1/2}^j(\theta) \sqrt{\eta_j}, \\ F_4 &= \sum_{j=1/2}^{\infty} (j + \frac{1}{2}) F_4^j d_{-1/2-1/2}^j(\theta) \sqrt{\eta_j}, \end{aligned} \quad (17)$$

where the factor $\sqrt{\eta_j}$ corrects the j th partial-wave channel for the absorption from the final $K^0\Sigma^+$ state. The absorption factor for the j th partial wave is obtained by substituting for the impact parameter by the classical-wave prescription

$$b \rightarrow \frac{l}{q} = \frac{j - \frac{1}{2}}{q}; \quad \eta_j = \left(1 - \frac{\sigma_i}{4\pi A} e^{-(j-\frac{1}{2})^2 2.24 q^2} \right). \quad (18)$$

Since many partial waves contribute at the high energies of interest, little error is introduced by using (18) for all j values in (17). We also neglect spin dependence in the absorption.

We have inserted (18) into (17) and added up the contributions for each j . The results are presented in Figs. 4 and 5 for two different photon energies, 10 and 15 BeV, [Figs. 3 and 4 give the differential cross section at 10 BeV] in the center-of-mass and laboratory systems. Shown in these figures are the Born-approximation results given in the high-energy and small-angle limit by (8), together with the curves showing successive reduction of the individual partial waves. Moreover, since we are interested in a lower bound in the production process in computing the secondary K_2 beam intensities, we choose $\sigma_i/4\pi A = 1$ corresponding to maximum S -wave absorption. In Fig. 6 the actual parameters of (12) were used in evaluating (18).

⁷ M. Jacob and G. C. Wick, Ann. Phys. (N. Y.) 7, 404 (1949).

The coupling constants used have been obtained in the following way: SU_3 symmetry⁸ relates the $K^*\rho\Sigma$ and ρ -nucleon coupling constants; namely

$$g_{K^*\rho\Sigma^+} = -\sqrt{2}g_{\rho^0pp}. \quad (19)$$

If the ρ meson is assumed to be coupled to the isotopic spin current one further has $g_{\rho^0pp} = \frac{1}{2}g_{\rho^0\pi^+\pi^+}$. With a ρ meson width of the order of 100 MeV, one takes

$$g_{K^*\rho\Sigma}^2/4\pi \approx 0.75. \quad (20)$$

The $K^*K\gamma$ and $\rho\pi\gamma$ coupling constants may be easily related by SU_3 symmetry if the electromagnetic current transforms like a member of an octet. This gives $g_{K^*K^0\gamma} = -2g_{\rho^0\pi^0\gamma}$. The $\rho\pi\gamma$ coupling constant is then related to the ρ radiative decay width by (6) when the K^* and K masses are, respectively, replaced by the ρ and π masses. If Γ_γ stands for the ρ radiative decay width, in MeV, we have

$$g_{K^*K^0\gamma}/4\pi \approx 0.13\Gamma_\gamma. \quad (21)$$

The curves of Figs. 3, 4, 5, and 6 correspond to (20) and (21) with a ρ -meson radiative width of 0.15 MeV.

This is a conservative estimate as recently reported measurements⁹ of ρ^0 photoproduction, if interpreted as due entirely to one-pion exchange, lead to a ρ radiative width of 1.5 MeV, \sim ten times larger. Our results in Figs. 3, 4, 5, and 6 can be scaled simply by the ratio of the observed ρ radiative decay width to the assumed value of 0.15 MeV when data are available.

CONCLUSIONS

Before anyone is tempted to ascribe too much weight to the detailed numerical results we call attention to the fact that a representation of the diffraction scattering of a meson-baryon system by a purely imaginary amplitude, as done in (11), fails to reproduce the recently reported real part of the forward scattering amplitude.¹⁰ Also there is considerable latitude at present in our knowledge of the coupling constants $g_{K^*K\gamma}$ and $g_{K^*\rho\Sigma}$. The relatively large cross section, obtained from K^* exchange, is due to the fact that absorption, although strong, is mainly confined to the low partial waves ($j < 8$ at 15 BeV). An additional and noninterfering mechanism for photoproducing K^0 mesons is via the

⁸ M. Gell-Mann, California Institute of Technology Report CTSL-20, 1961 (unpublished).

⁹ H. R. Crouch, Jr., *et al.*, Phys. Rev. Letters **13**, 640 (1964). The ρ radiative width would be further increased if the one-pion exchange calculations to which the experiments are compared [S. M. Berman and S. D. Drell, Phys. Rev. **133**, B791 (1964)] are reduced by the analogous final-state corrections as discussed in this paper. More recent counter data on the energy dependence of ρ^0 photoproduction from hydrogen [F. Pipkin (private communication)] indicate the presence of the one-pion exchange in addition to the diffraction mechanism and support the use of 0.15 MeV as a conservative estimate of the ρ radiative decay width.

¹⁰ S. J. Lindenbaum, Rapporteur's talk, 1964 International Conference on High-Energy Physics, Dubna (unpublished).

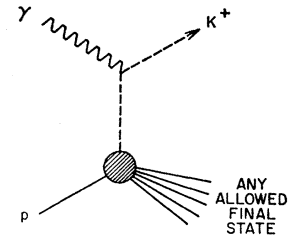


FIG. 7. K^+ photoproduction via K^+ exchange.

charged K^* current followed by the subsequent decay $K^{*+} \rightarrow K^0 + \pi^+$. As discussed in Ref. 9 this could be important at small angles if the charged K^* has a nonvanishing anomalous magnetic moment. There is also the additional cross section for the exchanged K^* in Fig. 1 to excite resonance and multiparticle final states in addition to the Σ^+ as shown.¹¹

Although the peak in the differential cross section for K^0 production increases approximately with the square of the photon energy, the cross section integrated over the peak width of $\approx \pi m^{*2}/k^2$ sr is constant, independent of energy. This may prove to be an over-optimistic extrapolation from the 4-BeV to the 15-BeV region if further experience shows that, in addition to the reduction due to absorption into competing channels, the vector K^* exchange should also be "Reggeized."¹² If so, it may help to erase at least part of the pessimism built into our calculations by our choice of parameters corresponding to maximum absorption and to a small ρ radiative decay width.

These results have to be compared to photoproduction of charged K mesons expected at the same energy. Assuming the electromagnetic current to transform like a member of an octet we use charge independence to obtain a ratio of $\frac{1}{2}$ between the $\gamma + p \rightarrow K^0\Sigma^0$, Λ^0 and $\gamma + p \rightarrow K^0\Sigma^+$ cross sections as computed above. We expect then a K^+ differential cross section of the order of 10 $\mu\text{b}/\text{sr}$ at the laboratory peak angle for an incident photon of 15 BeV due to K^* exchange. This is to be compared with a peak differential cross section of ≈ 100 $\mu\text{b}/\text{sr}$ expected from the K^+ current contribution which is illustrated in Fig. 7, when we include all inelastic final states that can be excited by the normalized equivalent quantum spectrum from an incident 20-BeV electron.

The numerical calculations were carried out on the Stanford B5000 computer. Results as plotted directly by the machine are shown in Fig. 3. It is a pleasure to thank S. Howry for an introduction to the Algol system.

¹¹ Whether or not the absorption factor, computed here to reduce the peak cross section by a factor of 10, is present for multiparticle final states is an open question. In the analogous situation for ρ production via one-pion exchange no reduction in cross section was observed up to energies of 18 BeV. [L. Jones, Phys. Rev. Letters **14**, 186 (1965).]

¹² In the present calculation a decrease in the cross section with energy can be found only if the diffraction peak becomes less broad at higher energies.